34th Annual International Conference of the IEEE EMBS
San Diego, California USA, 28 August - 1 September, 2012

Diffusion kurtosis imaging with tract-based spatial statistics reveals white matter alterations in preschool children

Xianjun Li [1,2], Jie Gao [1], Xin Hou[1], Kevin C. Chan[3,4], Abby Ding[3], Qinli Sun[1], Mingxi Wan [2], Ed X. Wu[3], and Jian Yang [1,2*]

1. Department of Radiology, the First Affiliated Hospital of Medical College of Xi'an Jiaotong University, Xi'an, China.
2. Department of Biomedical Engineering, School of Life Science and Technology, Xi'an Jiaotong University, Xi'an, China.
3. Laboratory of Biomedical Imaging and Signal Processing, The University of Hong Kong, Hong Kong SAR, China
4. Departments of Ophthalmology and Bioengineering; Center for the Neural Basis of Cognition, University of Pittsburgh, Pittsburgh, PA,

Abstract— **Diffusion kurtosis imaging (DKI), an extension of diffusion tensor imaging (DTI), provides a practical method to describe non-Gaussian water diffusion in neural tissues. The sensitivity of DKI to detect the subtle changes in several chosen brain structures has been studied. However, intuitive and holistic methods to validate the merits of DKI remain to be explored. In this paper, tract-based spatial statistics (TBSS) was used to demonstrate white matter alterations in both DKI and DTI parameters in preschool children (1-6 years; n=10). Correlation analysis was also performed in multiple regions of interest (ROIs). Fractional anisotropy, mean kurtosis, axial kurtosis and radial kurtosis increased with age, while mean diffusivity and radial diffusivity decreased significantly with age. Fractional anisotropy of kurtosis and axial diffusivity were found to be less sensitive to the changes with age. These preliminary findings indicated that TBSS could be used to detect subtle changes of DKI parameters on the white matter tract. Kurtosis parameters, except fractional anisotropy of kurtosis, demonstrated higher sensitivity than DTI parameters. TBSS may be a convenient method to yield higher sensitivity of DKI.**

Index Terms— **Diffusion kurtosis imaging (DKI), tract-based spatial statistics (TBSS), white matter, preschool children**

I. INTRODUCTION

Diffusion kurtosis imaging (DKI) was proposed to describe the deviation of water diffusion in biological tissues from Gaussian diffusion [1-3]. As an extension of diffusion tensor imaging (DTI), DKI characterizes the restricted diffusion environment [4], while DTI indicates the degree of water diffusion. Similar to the 2nd order diffusion tensor (DT) in DTI, the 4th order diffusion kurtosis tensor (KT) can also be orthogonally transformed to compute the directional kurtosis [4, 5].

The sensitivity of DKI has been evaluated in several chosen brain structures [6, 7]. Mean kurtosis (*MK*) can provide more information to characterize age-related diffusion changes in developing and aging brains than that obtained from DTI [6]. Directional DKI parameters hold higher sensitivity than those of DTI [7]. However, there is no study to validate the merits of DKI using intuitive and holistic methods.

In DTI studies, tract-based spatial statistics (TBSS) provides a powerful and objective method to perform multi-subject comparison [8]. This method has been applied to demonstrate the differences between preterm infants and term control to reveal the brain development [9]. TBSS seems to be suited to investigate the white matter characterization with DKI as well [10]. DTI parameters change quickly during the first two years. Though the rate of changes slows down after two years old, the changes can be detected by fractional anisotropy (*FA*) [11-13]. The subtle changes may also be investigated by DKI with TBSS.

In this study, white matter alterations of both DKI and DTI parameters in preschool children were investigated using TBSS. The comparisons between DKI and DTI parameters were analyzed on the tract of the white matter. Four regions of interest (ROIs) in whiter matter were also studied to validate the efficiency of TBSS.

II. MATERIALS AND METHODS

A. Theory

In DKI, the signal attenuation model has the expansion [1-3]:

$$\ln[s(b)/s(0)] \approx -bD_{app} + (1/6)b^2 D_{app}^2 K_{app}. \qquad (1)$$

where D_{app} is the apparent diffusion coefficient, and K_{app} is the apparent kurtosis coefficient. DKI model was more accurate than DTI for signal fitting (especially for b-values higher than 1000 s/mm^2) [7, 14].

The 4th order diffusion kurtosis tensor (KT) can be orthogonally transformed by [4, 5]:

$$\hat{W}_{ijkl} = \sum_{i'=1}^{3}\sum_{j'=1}^{3}\sum_{k'=1}^{3}\sum_{l'=1}^{3} e_{i'i}e_{j'j}e_{k'k}e_{l'l}W_{i'j'k'l'}, \qquad (2)$$

where e_{ij} are the elements of the 3D rotate matrix. After computing the mean diffusivity (*MD*), axial diffusivity ($\lambda_{//}$), and radial diffusivity ($\lambda_{\perp}$), the kurtosis along the DT eigenvector direction can be derived [4, 5]:

$$K_i = (MD^2/\lambda_i^2)\hat{W}_{iiii}, \qquad (3)$$

This work was supported by the grant from National Natural Science Foundation of China (No.81171317 & No.30970797 to Jian Yang) and the 2011 New Century Excellent Talent Support Plan from Ministry of Education of China to Jian Yang.

*Jian Yang is with the Department of Radiology, the First Affiliated Hospital of Medical College of Xi'an Jiaotong University, Xi'an, Shannxi, People's Republic of China. (The corresponding author to provide phone: 086-029-85323643; fax: 086-029-85225009; e-mail: yj1118@mail.xjtu.edu.cn).

where $MD = (1/3)\sum_{i=1}^{3}\lambda_i$, λ_i are the eigenvalues of the DT.

The *MK*, axial kurtosis ($K_{//}$), radial kurtosis ($K_{\perp}$), and fractional anisotropy of kurtosis (FA_K) can be computed as follows [4, 5]:

$$MK = (1/n)\sum_{i=1}^{n}(K_{app})_i \,, \tag{4}$$

$$K_{//} = K_1 \,, \tag{5}$$

$$K_{\perp} = (K_2 + K_3)/2 \,, \tag{6}$$

$$FA_K = \sqrt{\frac{3}{2}\cdot\frac{(K_1-\overline{K})^2+(K_2-\overline{K})^2+(K_3-\overline{K})^2}{K_1^2+K_2^2+K_3^2}} \,, \tag{7}$$

where $\overline{K} = (1/3)\sum_{i=1}^{3}K_i$.

B. Subjects

Ten healthy preschool children (3 girls, 7 boys; mean age = 3.2 ± standard deviation (SD) = 1.9 years; age range: 1-6 years) were studied in this study. All parents of children were informed with the goals and risks of MR scanning and requested written consent before enrollment. Children who were confirmed or suspected to have congenital malformations of central nervous system, congenital infections, metabolic disorders, hydrocephalus or brain injuries caused by any diseases, abnormal conventional MR appearances were all excluded from this study.

The children were divided into two groups: group one (age range: 1-3 years; n=6) and group two (age range: 4-6 years; n=4). All studies were approved by the local institutional board.

C. Data acquisition

The children were all sedated oral chloral hydrate (25 - 50 mg/kg) before scanning. The three-dimensional magnetization prepared rapid gradient echo (3D-MPRAGE) T1WI, fast spin echo (FSE) T2WI, and DKI by single short echo planar sequence were performed in a 3T scanner (Signa HDxt, General Electric Medical System, Milwaukee, WI, USA) with 8-channel high-resolution radio-frequency head coil. DKI was carried out by 25 directions, SENSE factor = 2, TR/TE = 4000/106.6 ms, slice thickness = 5 mm without gap, field of view = 180 ×180 mm^2, matrix = 128 × 128 (voxel size = 1.41 × 1.41 × 5 mm^3), b value = 500, 1000, 1500, 2000, 2500 s/mm^2. DKI scan time: 8 min 44 s.

D. Data analysis

The diffusion-weighted images were first co-registered to b0 using automated image registration (AIR5.2.5) [15]. MATLAB (Mathworks, Natick, MA, USA) was used to calculate *FA*, *MD*, $\lambda_{//}$, $\lambda_{\perp}$, FA_K, *MK*, $K_{//}$, $K_{\perp}$ [4, 5, 16].

The statistics analysis of DKI data was performed using TBSS [8] from a part of FMRIB's Software Library (FSL) [17]. Extracted brain images were acquired using Brain Extraction Tool (BET, package in the FSL) [18]. Before the nonlinear registration, linear registration was used to register every subject's *FA* image to each other [19]. TBSS was used to align all subjects' *FA* images to the target image (the representative *FA* image) and affine the aligned images into 1 × 1 × 1 mm^3 MNI152 standard space. An average *FA* image was created. Then the average *FA* image was used as the target image for the next step. Another registration was performed to register all subjects' *FA* images to the second target image. The aligned *FA* images were then used to create mean *FA* and mean *FA* skeleton. Each subject's aligned *FA* image was projected onto the mean *FA* skeleton (threshold = 0.2) before applying voxel-wise cross-subject statistics. The differences of *FA*, *MD*, $\lambda_{//}$, $\lambda_{\perp}$, FA_K, *MK*, $K_{//}$, and $K_{\perp}$ on the skeletons between groups were tested. The results were fully corrected for multiple comparisons across space using threshold free cluster enhancement (TFCE). All tests were considered to be significant at $p<0.05$.

ROIs were manually drawn using FSLVIEW (part of FSL). Four ROIs were defined, including genu of corpus callosum (GCC), splenium of corpus callosum (SCC), anterior limb of internal capsule (ALIC), and posterior limb of internal capsule (PLIC). Spearman-rho and linear regression analysis were performed to test the correlation between DTI, DKI parameters and age using MATLAB.

III. RESULTS

A. Comparison between DKI and DTI using TBSS

Figure 1 showed the significant differences of *FA*, FA_K, *MD*, *and MK* on the main part of white matter between the group 1 and group 2 in TBSS maps. Similarly, Figure 2 illustrated the TBSS results of directional diffusivity and kurtosis. In Figure 1, significant increase of FA was found mainly in GCC, body of corpus callosum, and PLIC. Though the same areas were also shown on FA_K, the areas on FA_K were illustrated in red to yellow without TFCE-correction. *MD* decreased and *MK* increased significantly in almost all the skeleton of white matter, except SCC. Note that *MK* exhibited relatively higher sensitivity in GCC and some peripheral skeleton than that of *MD*. In Figure 2, even though the test of $\lambda_{//}$ was not corrected, fewer changes were found. Compared with $\lambda_{//}$, significant increase of $K_{//}$ was observed. In the radial direction, $\lambda_{\perp}$ decreased and $K_{\perp}$ increased significantly with age in the main part of white matter between the group 1 and group 2 in TBSS maps. Moreover, $K_{\perp}$ was more sensitive than $\lambda_{\perp}$ to detect the change in GCC and some peripheral skeleton.

In TBSS, the deviation of T-statistics from zero indicates the degree of the difference between groups. Figure 3 showed the normalized histogram of T-statistics value. The largest deviation of the T-statistics from zero was found in *MK*. FA_K held the smallest deviation. Compared with DTI parameters, greater deviations of DKI parameters, except for FA_K, were shown.

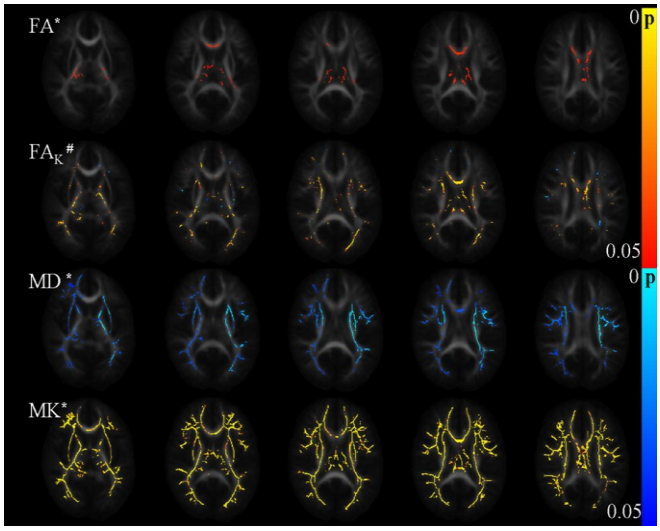

Figure 1. Comparisons of FA, FA_K, MD, MK between younger childern (1 – 3 years old) and older children (4 – 6 years old) on five axial slices (viewing left = anatomical right). Red to yellow regions show the areas where the parameters increased with age. Blue regions show the areas where the parameters decreased with age. *: TFCE-corrected; #: uncorrected.

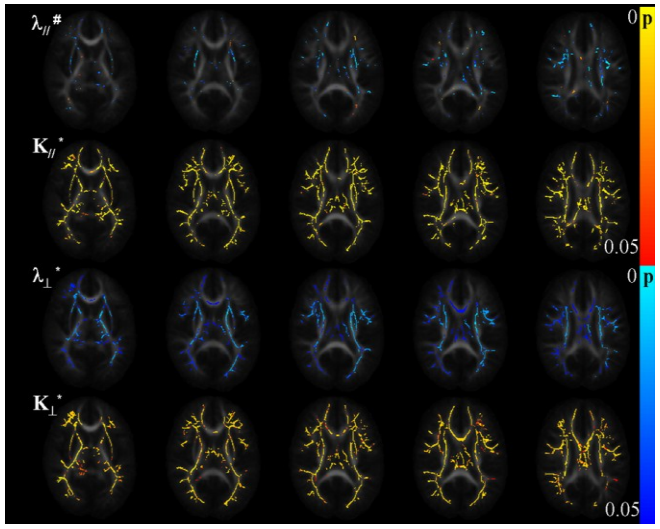

Figure 2. Comparisons of $\lambda_{//}$, $K_{//}$, $\lambda_{\perp}$, $K_{\perp}$ between younger childern (1 – 3 years old) and older children (4 – 6 years old) on five axial slices (viewing left = anatomical right). Red to yellow regions show the areas where the parameters increased with age. Blue regions show the areas where the parameters decreased with age. *: TFCE-corrected; #: uncorrected.

B. Comparison between DKI and DTI in ROIs

The results of correlation analysis between DTI, DKI parameters and age are listed in TABLE I. In GCC, ALIC, and PLIC, FA_K had a weaker correlativity than FA with age. The correlation between MK and age was stronger than that between MD and age in all the four ROIs. $K_{//}$ had a greater correlativity than $\lambda_{//}$ with age in GCC, ALIC, and PLIC. In GCC, SCC, and ALIC, the correlation between $K_{\perp}$ and age was stronger, compared with the correlation between $\lambda_{\perp}$ and age. In TABLE I, the slope of the correlation curve can be used to character the change rate of DTI and DKI parameters over time. In all the four ROIs, MK changed more markedly than MD; $K_{\perp}$ varied more markedly than $\lambda_{\perp}$. $K_{//}$ varied more obviously than $\lambda_{//}$ in GCC, ALIC, and PLIC. Compared with FA, FA_K changed more obviously in GCC, SCC, and PLIC.

IV. DISCUSSIONS

In conventional DTI, diffusivity cannot fully characterize the subtle changes of developmental white matter. DKI-derived parameters, including diffusivity and kurtosis,

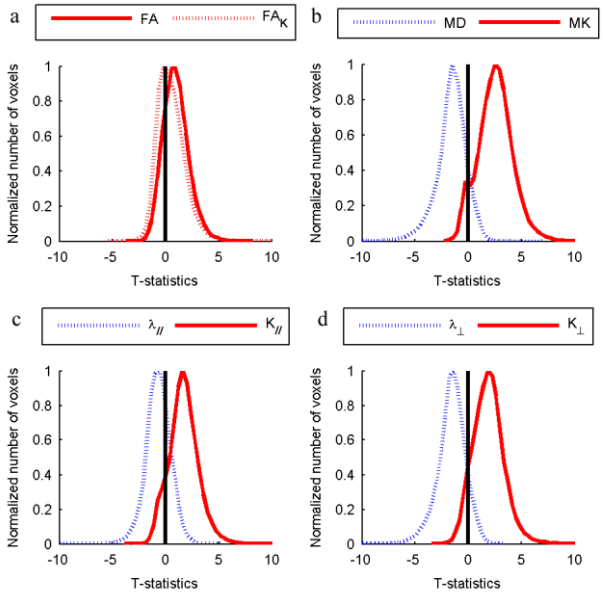

Figure 3. Normalized histogram of T-statistics in TBSS. Red: $group_{4\text{-}6\ years} > group_{1\text{-}3\ years}$; Blue: $group_{4\text{-}6\ years} < group_{1\text{-}3\ years}$.

TABLE I. CORRELATIONS BETWEEN DTI, DKI PARAMETERS AND AGE

		GCC	SCC	ALIC	PLIC
r	FA	0.59	0.09	0.61	0.86*
	FA_K	0.43	0.15	0.32	0.61
	MD	-0.41	-0.01	-0.52	-0.52
	MK	0.83*	0.40	0.87*	0.75*
	$\lambda_{//}$	0.35	0.19	-0.08	0.24
	$K_{//}$	0.71*	0.12	0.85*	0.69*
	$\lambda_{\perp}$	-0.59	-0.13	-0.70*	-0.89*
	$K_{\perp}$	0.78*	-0.20	0.88*	0.77*
|b| ($\times 10^{-2}$)	FA	3.25	0.13	1.61	1.77
	FA_K	4.15+	0.36+	0.58	3.52+
	MD	2.81	0.11	1.14	1.20
	MK	6.58+	1.83+	4.07+	2.83+
	$\lambda_{//}$	1.12	0.50	0.36	0.95
	$K_{//}$	1.97+	0.09	2.95+	1.40+
	$\lambda_{\perp}$	4.77	0.09	1.89	2.27
	$K_{\perp}$	21.63+	1.40+	6.32+	6.33+

r: Spearman correlation coefficient.
b: Slope of the linear correlation curve.
+: $|b_{DKI\ parameter}| > |b_{DTI\ parameter}|$;
*: $p<0.05$.

can obtain more sensitive and specific characterizations in analysis of brain development [7]. Even after the age of 2 years old, human brain undergoes microstructural changes [11-13]. In current study, white matter alterations in preschool children were investigated.

During brain development, more diffusion restriction appears with age [20]. Therefore, as a direct index to detect

diffusion restriction, MK increased significantly. This may be one of the factors leading to the decrease of *MD*. The reduction of water content may also influence the change pattern of *MD*. By comparison between *MK* and *MD*, *MK* was more specific and sensitive to investigate developmental variations in white matter.

There are counteracting physiological changes on the axial direction. With an increase in the number and alignment of fibers countered by a reduction in total water, few significant changes of $\lambda_{//}$ were found in preschool children. The significant increase in $K_{//}$ may reflect the increase of restriction in axial direction. The results demonstrated that $K_{//}$ held higher level of significance in detecting the changes along the axons than $\lambda_{//}$.

As the thickness of myelin sheath and axonal caliber increases, the restriction in radial direction increases. This may be the main reason why $\lambda_{\perp}$ decreased and $K_{\perp}$ increased significantly. Higher sensitivity of $K_{\perp}$ may be a result of diffusion restriction from the developmental changes mainly in radial direction [7].

Both the TBSS and the ROI results showed that *FA* increased with age in internal capsule and GCC. However, no significant changes of FA_K were observed. The results indicated that there were no obvious changes in the anisotropy of directional restrictions during 1 to 6 years in preschool children.

In current study, brains of subjects from 1 to 6 years old of age were registered to a common template. The size difference of brains may influence the accuracy of registration. Though merits of DKI in detecting gray matter changes were not revealed here because of the limitation of TBSS, the sensitivity of DKI was validated objectively in this preliminary study. More detailed developmental changes of DKI parameters are to be investigated by further study with a larger population size. TBSS with DKI may also be a powerful method to investigate subtle variations of white matter in pathological analysis.

V. Conclusion

TBSS analysis was employed to investigate the changes of DKI parameters in preschool children for the first time. In this study, *MD*, $\lambda_{//}$, $\lambda_{\perp}$ decreased with age. *FA* and all the kurtosis parameters (FA_K, *MK*, $K_{//}$, $K_{\perp}$) increased with age. The results showed that TBSS with DKI could reveal the subtle changes of white matter in preschool children. *MK*, $K_{//}$, $K_{\perp}$ were more sensitive than *MD*, $\lambda_{//}$, $\lambda_{\perp}$. DKI with TBSS may be effective to provide specific information in human brain development study.

Acknowledgments

The authors would like to thank Drs. He Wang, Zhikui Xiao and Guang Cao from Applied Science Lab, GE Healthcare for their technical assistance.

References

[1] J. Jensen and J. Helpern, "Quantifying non-Gaussian water diffusion by means of pulsed-field-gradient MRI," in Book Quantifying non-Gaussian water diffusion by means of pulsed-field-gradient MRI, vol. 11, *Series Quantifying non-Gaussian water diffusion by means of pulsed-field-gradient MRI*, Editor ed.^eds., City, 2003, pp. 2154.

[2] J.H. Jensen, J.A. Helpern, A. Ramani, H. Lu, and K. Kaczynski, "Diffusional kurtosis imaging: The quantification of non- gaussian water diffusion by means of magnetic resonance imaging," *Magnetic Resonance in Medicine*, vol. 53, no. 6, pp. 1432-1440, Jun. 2005.

[3] H. Lu, J.H. Jensen, A. Ramani, and J.A. Helpern, "Three- dimensional characterization of non- gaussian water diffusion in humans using diffusion kurtosis imaging," *NMR in Biomedicine*, vol. 19, no. 2, pp. 236-247, Apr. 2006.

[4] E.S. Hui, M.M. Cheung, L. Qi, and E.X. Wu, "Towards better MR characterization of neural tissues using directional diffusion kurtosis analysis," *Neuroimage*, vol. 42, no. 1, pp. 122-134, Aug. 2008.

[5] L. Qi, Y. Wang, and E.X. Wu, "D-eigenvalues of diffusion kurtosis tensors," *Journal of Computational and Applied Mathematics*, vol. 221, no. 1, pp. 150-157, Nov. 2008.

[6] M.F. Falangola, J.H. Jensen, J.S. Babb, C. Hu, F.X. Castellanos, A. Di Martino, S.H. Ferris, and J.A. Helpern, "Age- related non- Gaussian diffusion patterns in the prefrontal brain," *Journal of Magnetic Resonance Imaging*, vol. 28, no. 6, pp. 1345-1350, Dec. 2008.

[7] M.M. Cheung, E.S. Hui, K.C. Chan, J.A. Helpern, L. Qi, and E.X. Wu, "Does diffusion kurtosis imaging lead to better neural tissue characterization? A rodent brain maturation study," *Neuroimage*, vol. 45, no. 2, pp. 386-392, Apr. 2009.

[8] S.M. Smith, M. Jenkinson, H. Johansen-Berg, D. Rueckert, T.E. Nichols, C.E. Mackay, K.E. Watkins, O. Ciccarelli, M.Z. Cader, and P.M. Matthews, "Tract-based spatial statistics: voxelwise analysis of multi-subject diffusion data," *Neuroimage*, vol. 31, no. 4, pp. 1487-1505, Jul. 2006.

[9] M. Anjari, L. Srinivasan, J.M. Allsop, J.V. Hajnal, M.A. Rutherford, A.D. Edwards, and S.J. Counsell, "Diffusion tensor imaging with tract-based spatial statistics reveals local white matter abnormalities in preterm infants," *Neuroimage*, vol. 35, no. 3, pp. 1021-1027, Apr. 2007.

[10] E. Fieremans, J.H. Jensen, and J.A. Helpern, "White matter characterization with diffusional kurtosis imaging," *Neuroimage*, Sep. 2011.

[11] P. McGraw, L. Liang, and J.M. Provenzale, "Evaluation of normal age-related changes in anisotropy during infancy and childhood as shown by diffusion tensor imaging," *American Journal of Roentgenology*, vol. 179, no. 6, pp. 1515-1522, Dec. 2002.

[12] L. Hermoye, C. Saint-Martin, G. Cosnard, S.K. Lee, J. Kim, M.C. Nassogne, R. Menten, P. Clapuyt, P.K. Donohue, and K. Hua, "Pediatric diffusion tensor imaging: normal database and observation of the white matter maturation in early childhood," *Neuroimage*, vol. 29, no. 2, pp. 493-504, Jan. 2006.

[13] D. Ben Bashat, V. Kronfeld-Duenias, D.A. Zachor, P.M. Ekstein, T. Hendler, R. Tarrasch, A. Even, Y. Levy, and L. Ben Sira, "Accelerated maturation of white matter in young children with autism: a high b value DWI study," *Neuroimage*, vol. 37, no. 1, pp. 40-47, Aug. 2007.

[14] J. Zhuo, S. Xu, J. Hazelton, R.J. Mullins, J.Z. Simon, G. Fiskum, and R.P. Gullapalli, "Diffusion kurtosis as an in vivo imaging marker for reactive astrogliosis in traumatic brain injury," *Neuroimage*, vol. 59, no. 1, pp. 467–477, Jan. 2012.

[15] R.P. Woods, S.T. Grafton, C.J. Holmes, S.R. Cherry, and J.C. Mazziotta, "Automated image registration: I. General methods and intrasubject, intramodality validation," *Journal of computer assisted tomography*, vol. 22, no. 1, pp. 139, Jan.-Feb. 1998.

[16] J. Veraart, D.H.J. Poot, W. Van Hecke, I. Blockx, A. Van der Linden, M. Verhoye, and J. Sijbers, "More accurate estimation of diffusion tensor parameters using diffusion kurtosis imaging," *Magnetic Resonance in Medicine*, vol. 65, no. 1, pp. 138-145, Jan. 2011.

[17] S.M. Smith, M. Jenkinson, M.W. Woolrich, C.F. Beckmann, T.E.J. Behrens, H. Johansen-Berg, P.R. Bannister, M. De Luca, I. Drobnjak, and D.E. Flitney, "Advances in functional and structural MR image analysis and implementation as FSL," *Neuroimage*, vol. 23, pp. S208-S219, 2004.

[18] S.M. Smith, "Fast robust automated brain extraction," *Human brain mapping*, vol. 17, no. 3, pp. 143-155, Nov. 2002.

[19] G. Ball, S.J. Counsell, M. Anjari, N. Merchant, T. Arichi, V. Doria, M.A. Rutherford, A.D. Edwards, D. Rueckert, and J.P. Boardman, "An optimised tract-based spatial statistics protocol for neonates: Applications to prematurity and chronic lung disease," *Neuroimage*, vol. 53, no. 1, pp. 94-102, Oct. 2010.

[20] E.X. Wu and M.M. Cheung, "MR diffusion kurtosis imaging for neural tissue characterization," *NMR in Biomedicine*, vol. 23, no. 7, pp. 836-848, Aug. 2010.